

Evaluating Deep Learning and Traditional Approaches Used in Source Camera Identification

Mansur Ozaman

Nazarbayev Intellectual School of Science and Mathematics
in Medeu District of Almaty

November 18, 2025

Abstract

One of the most important tasks in computer vision is identifying the device using which the image was taken, useful for facilitating further comprehensive analysis of the image. This paper presents comparative analysis of three techniques used in source camera identification (SCI): Photo Response Non-Uniformity (PRNU), JPEG compression artifact analysis, and convolutional neural networks (CNNs). It evaluates each method in terms of device classification accuracy. Furthermore, the research discusses the possible scientific development needed for the implementation of the methods in real-life scenarios.

Keywords: source camera identification, PRNU, JPEG artifacts, convolutional neural networks, deep learning, smartphone images, camera fingerprinting

1 Introduction

According to the World Bank Group's Global Findex Digital Connectivity Tracker (2025), 68% of adults worldwide own a smartphone [1]. Determining the source device of a digital image has become a crucial task in the context of such widespread smartphone usage. Smartphone users are able to tamper with images or post them in misleading contexts. Hence, source camera identification (SCI) should be used to analyze and track digital images, restoring their authenticity and credibility as sources of information. SCI is also important for the development of fields such as multimedia security and intellectual property protection. Moreover, as AI image-generating models continue to advance, strengthening SCI techniques has become essential for maintaining the integrity of digital media.

Traditional techniques used in SCI are based on sensor characteristics. More specifically, "in natural images, the dominant part of the pattern noise is the photo-response non-uniformity noise (PRNU). It is caused primarily by pixel non-uniformity (PNU), which is defined as different sensitivity of pixels to light caused by the inhomogeneity of silicon wafers and imperfections during the sensor manufacturing process" [2, p. 3]. Unique patterns inherent to each device are derived using mathematical formulas. The study will primarily focus on this pattern type when discussing traditional SCI techniques because of its ubiquity. Another class of features used in traditional SCI techniques derives from JPEG compression artifacts. Images saved in JPEG format undergo lossy compression that introduces patterns such as blocking and quantization noise. JPEG artifacts can be utilized for identifying the source of an image, particularly when metadata is stripped or images are heavily compressed before analysis [3].

As most images circulating online today are shared through social media, which removes metadata and allows users to modify visual features with filters (which distort the patterns used in image investigation), new convolutional neural network (CNN)-based techniques have emerged. These methods are often regarded as superior to traditional sensor-based approaches due to their ability to dynamically learn features from the data.

In this research, a comparative analysis of the three methods—PRNU, JPEG artifact analysis, and CNN—is presented based on their accuracy. Firstly, PRNU patterns are derived from an image dataset composed of images made by students using their smartphones. Secondly, JPEG compression artifacts are extracted from the same dataset and used for comparison. Finally, CNN-based methods are benchmarked, and conclusions on the relative accuracy of each method are drawn.

2 Methods

2.1 Dataset and Preprocessing

I evaluate three families of source camera identification methods on a dataset consisting of four smartphone devices: Xiaomi Redmi Note 10S, Samsung Galaxy S24, iPhone 13 Pro Max, and iPhone 17 Pro. The data directories are structured as `data/redminote10s/`, `data/samsungs24/`, `data/iphone13promax/`, and `data/iphone17pro/`. Redmi and Samsung images are stored as JPEG files, while both iPhone models provide images in HEIC (HEIF) format. The dataset used in this work is publicly available at [4].

All images are loaded using Python and decoded to RGB using Pillow [5] and pillow-heif [6], and converted to NumPy arrays [7].

For the JPEG artifact and PRNU-based pipelines, images are converted to grayscale using the standard ITU-R BT.601 luma transform. For the CNN classifier, the RGB images are resized to 128×128 pixels using bilinear interpolation and normalized to the $[0, 1]$ range by dividing by 255.

For each method I employ the same stratified 70/30 train-test split (stratified by device class) with a fixed random seed, to make the results directly comparable across the three methods. The code used to process and analyze the images is publicly available [8].

2.2 JPEG Artifact-Based Features

JPEG compression is block-based and operates by applying the two-dimensional discrete cosine transform (DCT) to non-overlapping 8×8 blocks, followed by scalar quantization and entropy coding [9]. Different camera models and firmware typically use different quantization tables and pre-processing steps, leading to distinct distributions of DCT coefficients which can be exploited for camera model identification [10].

Let I denote a grayscale image of size $H \times W$. To ensure an integer number of blocks I crop the image so that both dimensions are multiples of 8:

$$H' = H - (H \bmod 8), \quad W' = W - (W \bmod 8),$$

and retain only the top-left $H' \times W'$ region. The image is then partitioned into $M = (H'/8) \cdot (W'/8)$ non-overlapping blocks $\{b_m\}_{m=1}^M$, each of size 8×8 .

For each block b_m , I compute the 2D DCT according to

$$C_m(u, v) = \alpha(u)\alpha(v) \sum_{x=0}^7 \sum_{y=0}^7 b_m(x, y) \cos\left(\frac{(2x+1)u\pi}{16}\right) \cos\left(\frac{(2y+1)v\pi}{16}\right), \quad (1)$$

for $u, v = 0, \dots, 7$, with

$$\alpha(0) = \frac{1}{\sqrt{8}}, \quad \alpha(k) = \frac{1}{2}, \quad k = 1, \dots, 7.$$

I discard the DC coefficient $(u, v) = (0, 0)$ and focus on AC coefficients, which are more directly shaped by quantization. For each AC position $(u, v) \neq (0, 0)$, I compute the empirical mean and variance of the coefficient over all blocks:

$$\mu_{u,v} = \frac{1}{M} \sum_{m=1}^M C_m(u, v), \quad \sigma_{u,v}^2 = \frac{1}{M-1} \sum_{m=1}^M (C_m(u, v) - \mu_{u,v})^2. \quad (2)$$

The JPEG artifact feature vector \mathbf{f} is formed by concatenating all means and variances of the AC coefficients:

$$\mathbf{f} = [\{\mu_{u,v}\}_{(u,v) \neq (0,0)}, \{\sigma_{u,v}^2\}_{(u,v) \neq (0,0)}]^\top. \quad (3)$$

Before classification, each feature dimension is standardized to zero mean and unit variance. I then use a support vector machine (SVM) with a radial basis function (RBF) kernel [11] as the classifier, implemented using scikit-learn [12]. Even for HEIC images, the same pipeline is applied to the decoded grayscale image, so that all devices are processed uniformly in the spatial domain.

2.3 PRNU-Based Features

Photo Response Non-Uniformity (PRNU) originates from slight variations in pixel sensitivities on the image sensor. It can be modeled as [2]

$$I = I_0(1 + K) + \Theta, \quad (4)$$

where I is the observed image, I_0 is the ideal noise-free image, K is the PRNU pattern, and Θ summarizes other noise sources. PRNU can be obtained from a noise residual and used as a device-specific fingerprint.

I first convert the RGB image to grayscale, cast to floating point, and normalize intensities to $[0, 1]$. A high-frequency residual is extracted by subtracting a smoothed version of the image:

$$R = I - G_{\sigma_1} * I, \quad (5)$$

where G_{σ_1} is a Gaussian kernel with standard deviation σ_1 and $*$ denotes convolution.

To suppress non-PRNU components, I estimate local mean and variance of the residual using another Gaussian filter [2]:

$$\mu(x) = G_w * R(x), \quad (6)$$

$$\sigma^2(x) = G_w * R^2(x) - \mu^2(x), \quad (7)$$

and form a Wiener-style estimate

$$\hat{R}(x) = (R(x) - \mu(x)) \cdot \frac{\sigma^2(x)}{\sigma^2(x) + \sigma_n^2}, \quad (8)$$

with σ_n^2 a small constant. The PRNU-like pattern is then

$$K(x) = R(x) - \hat{R}(x). \quad (9)$$

The pattern K is flattened into a one-dimensional vector

$$\mathbf{g} = \text{vec}(K), \quad (10)$$

and, for computational convenience, a fixed subset of entries is retained as the final feature vector. As in the JPEG case, the features are standardized and fed into a linear SVM [12], following the approach used in large-scale PRNU-based camera identification [13].

2.4 CNN-Based Classifier

The third approach uses a convolutional neural network trained end-to-end on RGB images to directly learn features for camera identification, in the spirit of [14]. Each input image is resized to $128 \times 128 \times 3$ and scaled to the $[0, 1]$ range. The network architecture is implemented using TensorFlow [15] and Keras [16]:

1. A convolutional layer with 32 filters of size 3×3 , followed by ReLU activation and 2×2 max pooling.
2. A convolutional layer with 64 filters of size 3×3 , followed by ReLU activation and 2×2 max pooling.
3. A convolutional layer with 128 filters of size 3×3 , followed by ReLU activation.
4. A flatten layer.
5. A fully connected layer with 64 neurons and ReLU activation.
6. An output fully connected layer with 4 neurons (one per device class) and softmax activation.

For an input image \mathbf{X}_i , the final layer produces logits $z_{i,k}$ for each class $k \in \{1, \dots, 4\}$. The corresponding posterior probabilities are given by the softmax function

$$p_{i,k} = \frac{\exp(z_{i,k})}{\sum_{j=1}^4 \exp(z_{i,j})}. \quad (11)$$

Training uses the categorical cross-entropy loss

$$\mathcal{L} = -\frac{1}{N} \sum_{i=1}^N \sum_{k=1}^4 y_{i,k} \log p_{i,k}, \quad (12)$$

where N is the number of training samples and $y_{i,k}$ is the one-hot encoding of the ground-truth label of image i . The network is optimized using the Adam optimizer [17] for five epochs with mini-batches of size 8.

2.5 Evaluation Metric

For each method, classification performance is measured using the overall accuracy on the test set:

$$\text{Accuracy} = \frac{1}{N_{\text{test}}} \sum_{i=1}^{N_{\text{test}}} \mathbb{1}[\hat{y}_i = y_i], \quad (13)$$

where N_{test} is the number of test samples, y_i is the ground-truth device label, \hat{y}_i is the predicted label, and $\mathbb{1}[\cdot]$ is the indicator function. Normalized confusion matrices are also computed for each method using Matplotlib [18] and Seaborn [19]; each row corresponds to the true device and each column to the predicted device, with rows summing to one.

3 Results

3.1 Overall Classification Accuracy

Figure 1 summarizes the overall accuracy demonstrated by the three methods. The JPEG artifact-based classifier achieves the highest accuracy of $\text{Acc}_{\text{JPEG}} = 0.90$, followed by the PRNU-based classifier with $\text{Acc}_{\text{PRNU}} = 0.71$, while the CNN-based classifier reaches $\text{Acc}_{\text{CNN}} = 0.29$. This ranking shows a clear separation between the traditional feature approaches (JPEG and PRNU) and the end-to-end CNN classifier in this experimental setting. The JPEG method achieves the best overall performance and most clearly distinguishes between the four devices, while the PRNU method also captures a large part of the device-specific information but demonstrates more confusion between classes. Although the CNN method achieves significantly lower accuracy compared to the traditional methods, it still shows non-random patterns and thus can serve as a baseline for learned-feature comparison.

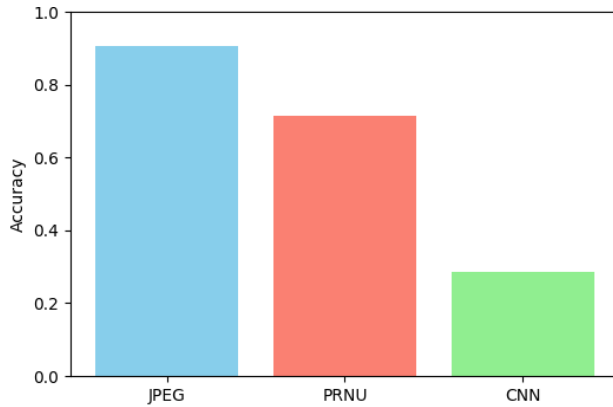


Figure 1: Overall accuracy comparison of the JPEG-based, PRNU-based, and CNN-based classification methods.

3.2 Per-Device Behaviour

To better understand the behavior of each method, I analyze the normalized confusion matrices shown in Figures 2 – 4. Each row corresponds to the true device name and each column to the predicted device (`iphone13promax`, `iphone17pro`, `redminote10s`, `samsungs24`).

JPEG Artifact-Based Classifier

Figure 2 shows that the JPEG classifier correctly labels all test images from `redminote10s` and `samsungs24` with a normalized accuracy of 1.00 on the corresponding diagonal entries. For the two iPhone models, the classifier perfectly recognises `iphone13promax` (diagonal entry 1.00) and classifies `iphone17pro` images less correctly, with 0.60 on the diagonal and 0.40 of these images assigned to `iphone13promax`. Thus, the JPEG-based approach is especially strong at separating devices that differ more strongly in their compression characteristics, while still providing good discrimination between the two related iPhone models.

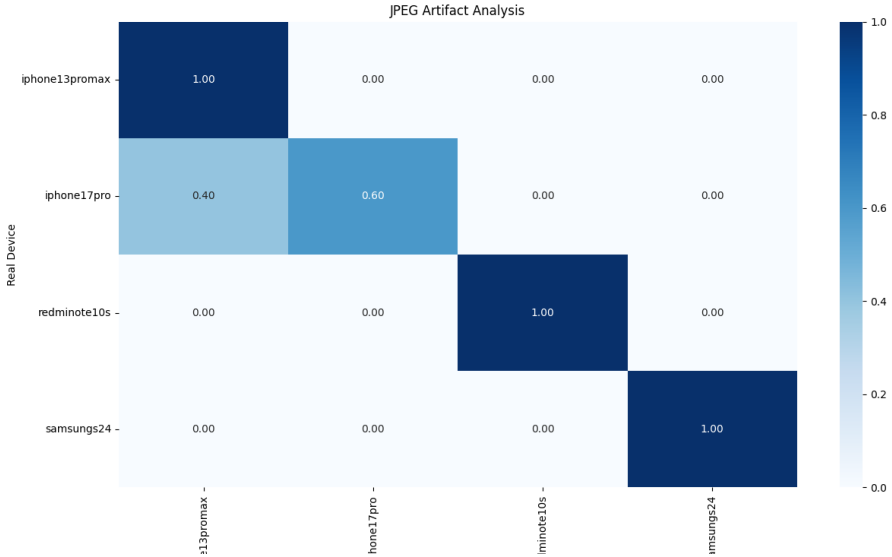


Figure 2: Confusion matrix for the JPEG artifact-based classifier.

PRNU-Based Classifier

The PRNU-based classifier (Figure 3) also achieves perfect recognition for the two Android devices: both `redminote10s` and `samsungs24` attain a normalized accuracy of 1.00 on the diagonal. For `iphone17pro`, 60% of the images are correctly identified, while 40% are assigned to `redminote10s`. For `iphone13promax`, the predictions are split between `iphone13promax` (0.20), `iphone17pro` (0.40), and `redminote10s` (0.40). Compared with the JPEG-based classifier, PRNU shows similarly strong performance on the Android devices but produces more mixing between the two iPhone classes and, to a lesser extent, between an iPhone and the Redmi device.

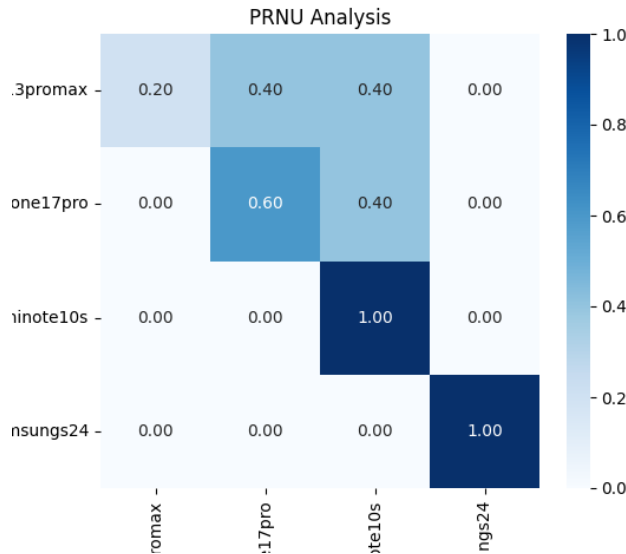


Figure 3: Confusion matrix for the PRNU-based classifier.

CNN Classifier

The CNN classifier (Figure 4) exhibits a distinctly different pattern. All `iphone13promax` test images are correctly predicted (diagonal entry 1.00), but all `iphone17pro` images are also

assigned to `iphone13promax`. For the Android devices, the majority of images from both `redminote10s` and `samsungs24` are mapped to the `iphone13promax` class (0.83 and 0.80 respectively), with only a small fraction of Android samples classified as `samsungs24`. This behaviour is consistent with the lower overall accuracy reported in Figure 1: the CNN captures some discriminative regularities that favour one dominant class but does not separate all four devices as clearly as the JPEG and PRNU-based methods.

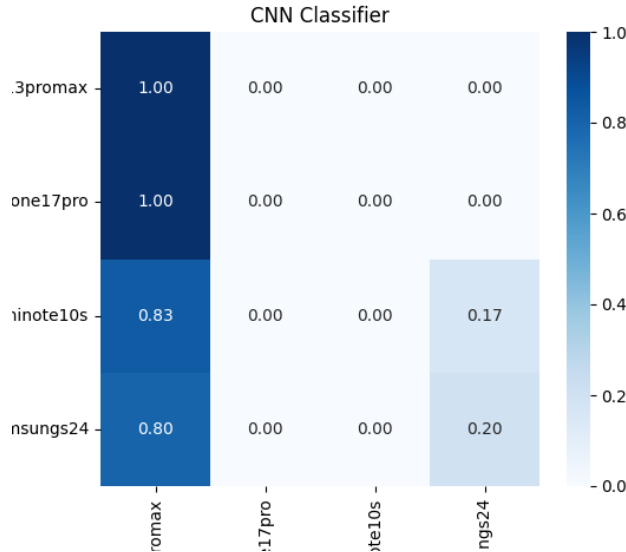


Figure 4: Confusion matrix for the CNN classifier.

3.3 Comparison of the Methods

Taken together, the results display a clear ranking of the methods. The JPEG artifact-based classifier shows the highest and most balanced performance across all four devices, with particularly strong results on Redmi and Samsung models. The PRNU-based classifier follows closely, matching JPEG performance on Redmi and Samsung devices and demonstrating competitive but less consistent results on the iPhone classes. The CNN classifier, used here as an end-to-end learned baseline, remains below both traditional approaches in overall accuracy and in the clarity of its device separation, largely favoring a single dominant class.

4 Conclusion

This work presented a comparative study of three source camera identification methods on a multi-device smartphone dataset: JPEG artifact-based features, PRNU fingerprint-based sensor noise analysis, and a convolutional neural network classifier. The JPEG artifact-based method achieved the highest overall accuracy of 0.90 and exhibited very clear device separation, especially for the two Android smartphones and for the iPhone 13 Pro Max. The PRNU-based method reached 0.71 accuracy and showed strong performance on the Android devices. By concentrating its predictions on a dominant class of images captured using the iPhone 13 Pro Max model, the CNN method showed an accuracy of 0.29 and a behaviour distinct from the other methods.

These results highlight the superiority of traditional, interpretable feature-based techniques over the CNN-based method. Future research can investigate hybrid approaches by combining the three aforementioned methods. Moreover, a larger dataset can be used to improve the research’s accuracy.

Acknowledgments

The author thanks the students who gave access to their smartphones for image collection. The author also thanks the developers of tools that were used in the computational work in this research, including NumPy [7], SciPy [20], scikit-learn [12], TensorFlow/Keras [15, 16], OpenCV [21], Matplotlib [18], Seaborn [19], Pillow [5], and pillow-heif [6].

References

- [1] World Bank Group. Global Findex Digital Connectivity Tracker 2025: Mobile phone technology powers saving surge in developing economies. July 16, 2025. <https://www.worldbank.org/en/news/press-release/2025/07/16/mobile-phone-technology-powers-saving-surge-in-developing-economies>.
- [2] J. Lukáš, J. Fridrich, and M. Goljan. Digital camera identification from sensor pattern noise. *IEEE Transactions on Information Forensics and Security*, 1(2):205–214, 2006.
- [3] M. J. Kwon, S. H. Nam, I. J. Yu, H. K. Lee, and C. Kim. Learning JPEG compression artifacts for image manipulation detection and localization. *International Journal of Computer Vision*, 130(8):1875–1895, 2022.
- [4] M. Ozaman, *edltauSCI Multi-Device Image Dataset*, Zenodo, 2025. <https://doi.org/10.5281/zenodo.17640511>. Accessed: 2025-11-18.
- [5] A. Clark and contributors. Pillow (PIL Fork) Documentation. 2023. <https://python-pillow.org>.
- [6] 0x646D and contributors. pillow-heif: A Python wrapper for libheif library. 2023. <https://github.com/0x646D/pillow-heif>.
- [7] C. R. Harris, K. J. Millman, S. J. van der Walt, et al. Array programming with NumPy. *Nature*, 585(7825):357–362, 2020.
- [8] M. Ozaman. *edltauSCI: Source Camera Identification Code*. GitHub repository, 2025. <https://github.com/ozxmn/edltauSCI>. Accessed: 2025-11-18.
- [9] G. K. Wallace. The JPEG still picture compression standard. *Communications of the ACM*, 34(4):30–44, 1991.
- [10] Z. Fan and R. L. de Queiroz. Identification of bitmap compression history: JPEG detection and quantizer estimation. In *Proceedings IEEE International Conference on Image Processing*, pages 3–6, 2000.
- [11] C. Cortes and V. Vapnik. Support-vector networks. *Machine Learning*, 20(3):273–297, 1995.
- [12] F. Pedregosa, G. Varoquaux, A. Gramfort, et al. Scikit-learn: Machine learning in Python. *Journal of Machine Learning Research*, 12:2825–2830, 2011.
- [13] M. Goljan, J. Fridrich, and T. Filler. Large scale test of sensor fingerprint camera identification. In *Media Forensics and Security*, Proc. SPIE 7254, 2009.
- [14] L. Bondi, L. Baroffio, D. Güera, P. Bestagini, E. J. Delp, and S. Tubaro. First steps toward camera model identification with convolutional neural networks. *IEEE Signal Processing Letters*, 24(3):259–263, 2017.

- [15] Martín Abadi, Ashish Agarwal, Paul Barham, et al. TensorFlow: Large-scale machine learning on heterogeneous systems, 2015. Software available from <https://www.tensorflow.org>.
- [16] F. Chollet et al. Keras. <https://keras.io>, 2015.
- [17] D. P. Kingma and J. Ba. Adam: A method for stochastic optimization. *arXiv preprint arXiv:1412.6980*, 2014.
- [18] J. D. Hunter. Matplotlib: A 2D graphics environment. *Computing in Science & Engineering*, 9(3):90–95, 2007.
- [19] M. L. Waskom. seaborn: statistical data visualization. *Journal of Open Source Software*, 6(60):3021, 2021.
- [20] P. Virtanen, R. Gommers, T. E. Oliphant, et al. SciPy 1.0: Fundamental algorithms for scientific computing in Python. *Nature Methods*, 17:261–272, 2020.
- [21] G. Bradski. The OpenCV Library. *Dr. Dobb's Journal of Software Tools*, 2000.